

# Influence of the demineralisation on the chemical activation of Kraft lignin with orthophosphoric acid

V. Fierro<sup>a,\*</sup>, V. Torné-Fernández<sup>b</sup>, A. Celzard<sup>c</sup>, D. Montané<sup>b</sup>

<sup>a</sup> *Laboratoire de Chimie du Solide Minéral, UMR CNRS 7555, Nancy-Université, BP 239, 54506 Vandœuvre-lès-Nancy, France*

<sup>b</sup> *Departament de Enginyeria Química, Universitat Rovira i Virgili, Avda dels Països Catalans, 26, 43007 Tarragona, Spain*

<sup>c</sup> *Laboratoire de Chimie du Solide Minéral, UMR CNRS 7555, Nancy-Université, ENSTIB, 27 rue du Merle Blanc, BP 1041, 88051 Épinal Cedex 9, France*

Received 5 December 2006; received in revised form 20 March 2007; accepted 20 March 2007

Available online 24 March 2007

## Abstract

The preparation of activated carbons (ACs) from the thermal decomposition of mixtures of orthophosphoric acid (PA) and either as-received softwood Kraft lignin, KL, or demineralised one, KL<sub>d</sub>, has been investigated. Activation with PA has been studied for a PA/lignin ratio of 1 (dry ash-free basis) and 1 h carbonisation time at final temperatures of 400, 500 and 600 °C. The yield, surface area, porosity, surface chemistry and methylene blue adsorption capacity have been determined. All ACs were found to be essentially microporous, with surface areas higher than 800 m<sup>2</sup>/g and a maximum value of nearly 1200 m<sup>2</sup>/g for the carbon prepared at 600 °C from KL. In order to study the influence of temperature on the properties of the ACs prepared from KL and KL<sub>d</sub>, the latter precursors were analysed by Fourier transform infrared spectroscopy (FT-IR), scanning electron microscopy (SEM) and X-ray diffraction (XRD). We have concluded that the very different characteristics of the ACs obtained from KL and KL<sub>d</sub> are due to the presence or not of mineral matter during carbonisation, but mainly to the demineralisation process itself, which produces polymerisation of the raw lignin. Methylene blue adsorption was found to be higher for ACs prepared from KL, mainly because of their higher ash and sulphur contents.

© 2007 Elsevier B.V. All rights reserved.

**Keywords:** Kraft lignin; Activated carbon; H<sub>3</sub>PO<sub>4</sub>; Demineralisation

## 1. Introduction

The Kraft method produces black liquor, a residue comprising lignin (30–40 wt.%) and other inorganic compounds, which is used as in-house fuel for the recovery of both energy and residual inorganic matter. An interesting alternative is the production of activated carbons by physical [1] or chemical activation [2–4].

Kraft lignin has a high content of inorganic/mineral matter that usually ranges from 6 to 15 wt.% on dry ash-free (daf) basis. Since the mineral matter does not directly contribute to the specific surface area and porosity of the resultant active carbons, it can be considered as an inert material which decreases the adsorption capacity per unit mass. The demineralisation and/or abatement of inorganic compounds from carbonaceous precursors are thus thought to be necessary for the production of porous

carbons with high surface areas [5]. This is particularly true for biomass, having higher inorganic contents than other precursors like synthetic polymers, and being recognised as a good feedstock for the production of cheap porous carbon materials. Thus, commercial activated carbons with low ash contents are prepared either by acid washing of the products, or by a suitable selection of the raw precursors [6]. Hence, in the case of precursors loaded with mineral matter, it may be wondered if the ashes should be removed before (i.e., in the precursor) or after (i.e., in the product) carbonisation and activation.

Indeed, it is well established that the presence of alkaline and alkaline earth elements in coals affects the reactivity of their chars, and that the catalytic effect of inorganic matter depends on their concentration, dispersion and chemical form in the coal matrix [7]. It is also the case with biomass, since Fengel and Wegener [8] suggested that the inorganic species naturally occurring in wood catalyse its pyrolysis. Since well-dispersed cations like sodium or calcium are helpful for activation of carbon by steam or CO<sub>2</sub> [9,10] and are abundant in lignin [11], a deminer-

\* Corresponding author. Tel.: +33 383684631; fax: +33 383684619.

E-mail address: [Vanessa.Fierro@lcsm.uhp-nancy.fr](mailto:Vanessa.Fierro@lcsm.uhp-nancy.fr) (V. Fierro).

alisation pre-treatment would be *a priori* harmful for obtaining efficient adsorbents.

It has been reported that sodium promotes demethoxylation, demethylation and dehydration of lignin [12,13], so the absence of such reactions could affect the final char yield. Furthermore, it has been recently shown [14] that, when lignin is demineralised from 5.7 to 1 wt.% and subsequently pyrolysed at 300 °C, the char yield decreases from ca. 71 to 51% (on a daf basis), respectively. Authors indicated that the partial removal of sodium and potassium enhanced the de-volatilisation of lignin at the expense of char formation. DeGroot and Shafizadeh [15] observed a similar decrease in the char yield of wood after acid-washing of the latter. However, the presence of inorganic matter in lignin was found to be useful in reducing its plasticity and hindering its swelling in the carbonisation stage when pyrolysed under N<sub>2</sub> atmosphere [1].

The growing interest in the use of wood and its derivatives for producing alternative fuels, chemicals and products of high added value, as activated carbons are, requires a fundamental understanding of the processes involved. Lignin, as a precursor of activated carbons, is the subject of an increasing number of papers [1–4,16–19] and, due to the high content of ashes in lignin, their effect on the pyrolysis process and on the carbonisation products is worth studying. In this work, the physico-chemical properties of activated carbons produced from the thermal decomposition of mixtures of orthophosphoric acid (PA) and either as-received Kraft lignin, KL, or demineralised one, KL<sub>d</sub>, were investigated.

## 2. Experimental

### 2.1. Precursor materials

Softwood Kraft lignin (KL) was supplied by Lignotech Iberica S.A. (Spain) in the form of fine dark brown particles. The inorganic matter was removed from KL as follows: batches of 100 g were introduced in 2 L of water, leading to black suspensions of pH 9.5. Lignin was precipitated by adding H<sub>2</sub>SO<sub>4</sub> until the pH decreased to 1. The precipitate was gently washed with distilled water until the pH of the rinse remained constant and close to 6, and finally dried overnight at 105 °C. The lignin prepared in this way was nearly mineral-free and was termed demineralised Kraft lignin (KL<sub>d</sub>).

### 2.2. Activated carbon preparation

An 85 wt.% H<sub>3</sub>PO<sub>4</sub> aqueous solution (Panreac, Spain) was used as activating agent. The weight ratio PA/precursor of all mixtures was 1.0 on a daf basis. The slurry was left for 1 h impregnation time at room temperature in air, then transferred into a furnace DUM Model 10CAF where carbonisation was carried out under air atmosphere. The furnace was heated at 10 °C/min, up to 150 °C, which temperature was held for 1 h to allow free evolution of water. Next, the oven was heated at 10 °C/min up to various carbonisation temperatures: 400, 500 and 600 °C, which were maintained for 1 h. The excess of H<sub>3</sub>PO<sub>4</sub> was removed after carbonisation by thorough washing with dis-

tilled water. As shown below, the resultant activated carbons were nearly free of ashes.

### 2.3. Characterisation of lignins and activated carbons

#### 2.3.1. Proximate and ultimate analysis

Analysis of C, H, S and N content in the activated carbons (ACs) was done using a Carlo Erba EA-1108 instrument, and oxygen was calculated by difference. The proximate analysis was carried out by thermogravimetric analysis in a Perkin-Elmer TGA 7 microbalance equipped with a 273–1273 K programmable temperature furnace. For that purpose, the weight losses were measured at 110 °C/air (moisture), 900 °C/non-oxidising atmosphere (volatile matter), 900 °C/air (fixed carbon). Ash content was obtained by difference.

#### 2.3.2. FT-IR analysis

Infrared spectra of KL, KL<sub>d</sub> and their derived ACs were recorded in the IR region (4000–600 cm<sup>-1</sup>) with a spectral resolution of 4 cm<sup>-1</sup>, a scan speed of 2 mm<sup>-1</sup> s<sup>-1</sup> and after 200 scans. The equipment used was a Fourier transform infrared (FT-IR) spectrophotometer JASCO FT/IR-680 equipped with a diamond-composite attenuated total reflectance (ATR) cell.

#### 2.3.3. SEM analysis

The surface morphology of KL and KL<sub>d</sub> was studied by scanning electron microscopy (SEM) with a JEOL JSM-6400. The microscope was equipped with an energy dispersive X-ray (EDX) microanalyser that was used to observe the dispersion of the mineral matter in KL and KL<sub>d</sub>.

#### 2.3.4. Surface area and porosity

Surface area and porosity were determined from the corresponding nitrogen adsorption–desorption isotherms obtained at 77 K with an automatic instrument (ASAP 2020, Micromeritics). The samples were previously outgassed at 523 K for several hours. N<sub>2</sub> adsorption data for relative pressures  $P/P_0$  ranging from 10<sup>-5</sup> to 0.99 (in a set of values previously fixed) were analysed according to: (i) the BET method for calculating the specific surface area,  $A_{BET}$ ; (ii) the Dubinin–Radushkevich (DR) for calculating the micropore volume,  $V_{DR}$ , the characteristic energy of N<sub>2</sub> with respect to carbon,  $E_0$ , and the average width of the slit-shaped micropores,  $L_0$ ; (iii) the  $\alpha_s$  method [20,21] for calculating the ultramicropore volume,  $V_{\alpha_{ultra}}$  and the micropore volume,  $V_{\alpha_{micro}}$ . The total pore volume,  $V_{0.99}$ , was calculated from nitrogen adsorption at a relative pressure of 0.99. The mesopore volume,  $V_{mp}$  was calculated as the difference between  $V_{0.99}$  and  $V_{DR}$ .

#### 2.3.5. Acidic groups titration

The total amount of acidic surface groups was determined as follows. About 25 mg of AC sample were placed in vials containing 25 mL of 0.05N aqueous solutions of sodium hydroxide. The vials were sealed and stirred for 48 h. Then, the solutions were filtrated, and 5 mL of each filtrate were taken off and titrated with 0.05N HCl. In order to achieve statistical soundness, at least three titrations were carried out for each sample. Average

values were therefore calculated, with typical errors being less than 10% of the reported averages.

### 2.3.6. Adsorption of methylene blue (MB)

MB is a standard compound frequently employed as a primary indicator of the adsorption capacity of AC<sub>S</sub> designed for removing organic pollutants from aqueous solutions. A calibration curve was first built by measuring the absorbance of aqueous solutions containing various amounts of MB, using an UV–vis 8500 Dinko Instruments spectrophotometer equipped with a tungsten lamp (working wavelength: 664.8 nm). Plotting the absorbance versus the MB concentration led to a straight line, thus allowing to quantify the presence of MB after having measured the absorbance of the investigated solution.

The analysis was performed as follows. About 33.7 mg of AC were introduced into a stoppered plastic bottle containing 50 mL of a solution which concentration in MB was  $3.2 \times 10^{-3}$  M. The resultant suspension was stirred for 24 h. The solution was subsequently filtered and analysed with the same UV–vis spectrophotometer. The MB concentration was deduced, and the adsorption capacity was calculated by the difference between the initial and the final concentration, and expressed in grams of MB per 100 g of activated carbon (g MB/100 g AC). Adsorption tests were repeated three times, with typical errors being less than 5% of the average value.

## 3. Results and discussion

### 3.1. Characterisation of KL and KL<sub>d</sub>

Table 1 shows the proximate and ultimate analyses of KL and KL<sub>d</sub>. It may be seen that the initial ash content of KL (11.1% dry basis) was nearly totally removed (0.2% dry basis) after the treatment with H<sub>2</sub>SO<sub>4</sub>. The high sulphur content (2.2%) in KL originates both from the Kraft or sulphate process, based on the action of NaOH and Na<sub>2</sub>S for separating cellulose from the other wood constituents, and from organically bound sulphur (up to 1.5%) [22]. XRD studies of lignin evidenced the presence of the phase Na<sub>2</sub>CO<sub>3</sub>·2Na<sub>2</sub>SO<sub>4</sub>, further confirmed by microprobe analysis. The demineralisation of lignin produced a decrease of both S (down to 0.5%) and O (from 33.3 to 27.8%) contents. This finding is not surprising since both sodium carbonate and sulphate are very soluble in aqueous solutions. Analysis by SEM–EDX showed that S and Na are uniformly distributed in the lignin before and after the demineralisation treatment.

Fig. 1 shows the IR spectra of KL and KL<sub>d</sub>. The two lignins show a broad band at 3000–3600 cm<sup>-1</sup>, attributed to the hydroxyl groups in phenolic and aliphatic structures, and

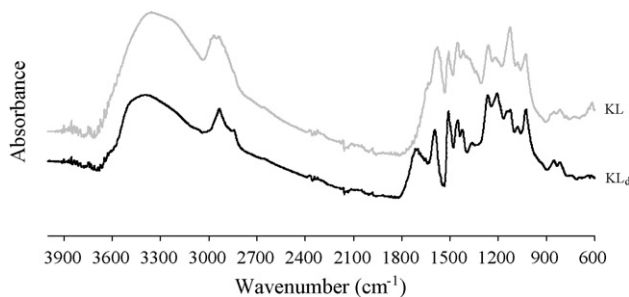


Fig. 1. FT-IR spectra of KL (grey line) and KL<sub>d</sub> (black line).

bands centred around 2975–2945 cm<sup>-1</sup>, predominantly arising from CH stretching in aromatic methoxyl groups and in methyl and methylene groups of side chains. Both bands decrease after acid treatment. The very small bands centred near 2300 cm<sup>-1</sup> are assigned to carbon–oxygen groups due to ketene [23].

The most characteristic infrared bands of lignin are found at about 1510 and 1600 cm<sup>-1</sup> (aromatic ring vibrations) and between 1470 and 1460 cm<sup>-1</sup> (C–H deformations and aromatic ring vibrations) [24]. The intensity of these bands, however, is strongly influenced by neighbouring functional groups.

In the KL spectrum, the band centred at 1585 cm<sup>-1</sup> is the result of aromatic ring vibrations at 1600 cm<sup>-1</sup> and coordinated carbonates [25], already evidenced by XRD analysis. The low absorption around 1650 cm<sup>-1</sup>, giving asymmetry and broadening to the more intense band at 1600 cm<sup>-1</sup>, may originate from both carbohydrates impurities and water associated with lignin [26]. Intense bands of the carbonyl groups appear in the range 1660–1725 cm<sup>-1</sup>. These bands are below or above 1700 cm<sup>-1</sup> if the C=O groups are conjugated with the aromatic ring or not, respectively.

After acid-washing, the carbonates are completely removed from lignin. Consequently, the intensity of the 1585 cm<sup>-1</sup> band decreases and is shifted to 1600 cm<sup>-1</sup>. The KL<sub>d</sub> spectrum also exhibits an intense band centred on 1729 cm<sup>-1</sup>, corresponding to C=O (ketones, aldehydes or carboxyl) groups not associated with aromatic rings.

The spectral region below 1400 cm<sup>-1</sup> is more difficult to analyse, since most bands are complex, with contribution from various vibration modes. However, this region contains vibrations that are specific to the different monolignol units and allows the structural characterisation of lignins. The spectra of both KL and KL<sub>d</sub> samples show the characteristic vibrations of the guaiacyl unit (1269 cm<sup>-1</sup>: guaiacyl ring breathing and C=O stretching; 1140 cm<sup>-1</sup>: C–H in-plane deformation; 860 and 824 cm<sup>-1</sup>: C–H out-of-plane vibrations in position 2, 5 and 6 of

Table 1  
Proximate and ultimate analyses of KL and KL<sub>d</sub> (wt.%)

	Proximate analysis (wt.%, dry basis)			Ultimate analysis (wt.%, daf)				
	Fixed carbon	Volatile matter	Ash	C	H	N	S	O <sup>a</sup>
KL	36.4	52.5	11.1	59.5	5.1	0.1	2.2	33.3
KL <sub>d</sub>	39.7	60.1	0.2	65.8	5.9	0.0	0.5	27.8

<sup>a</sup> Estimated by difference.

guaiacyl units), but the intensities of the bands vary significantly with the samples. The importance of guaiacyl characteristic vibrations increased after acid washing.

Both spectra also show a small band at  $1369\text{ cm}^{-1}$  due to phenolic OH and aliphatic C–H in methyl groups, and a strong vibration at  $1215\text{--}1220\text{ cm}^{-1}$  that can be associated with C–C plus C–O plus C=O stretching. The aromatic C–H deformation at  $1031\text{ cm}^{-1}$  appears as a complex vibration associated with the C–O, C–C stretching and C–OH bending in polysac-

charides. Carbohydrates that remained in KL could be also the cause of the vibrations in the spectral region  $1000\text{--}1300\text{ cm}^{-1}$  [26].

In summary, the most important changes introduced by acid-washing is the reduction of the amount of hydroxyl groups with the concomitant increase of the number of C=O functions, as well as the elimination of carbonates. In agreement with these findings, Yasuda et al. [27,28] demonstrated that the acid treatment of lignin produces its cross-linking, an increase of the

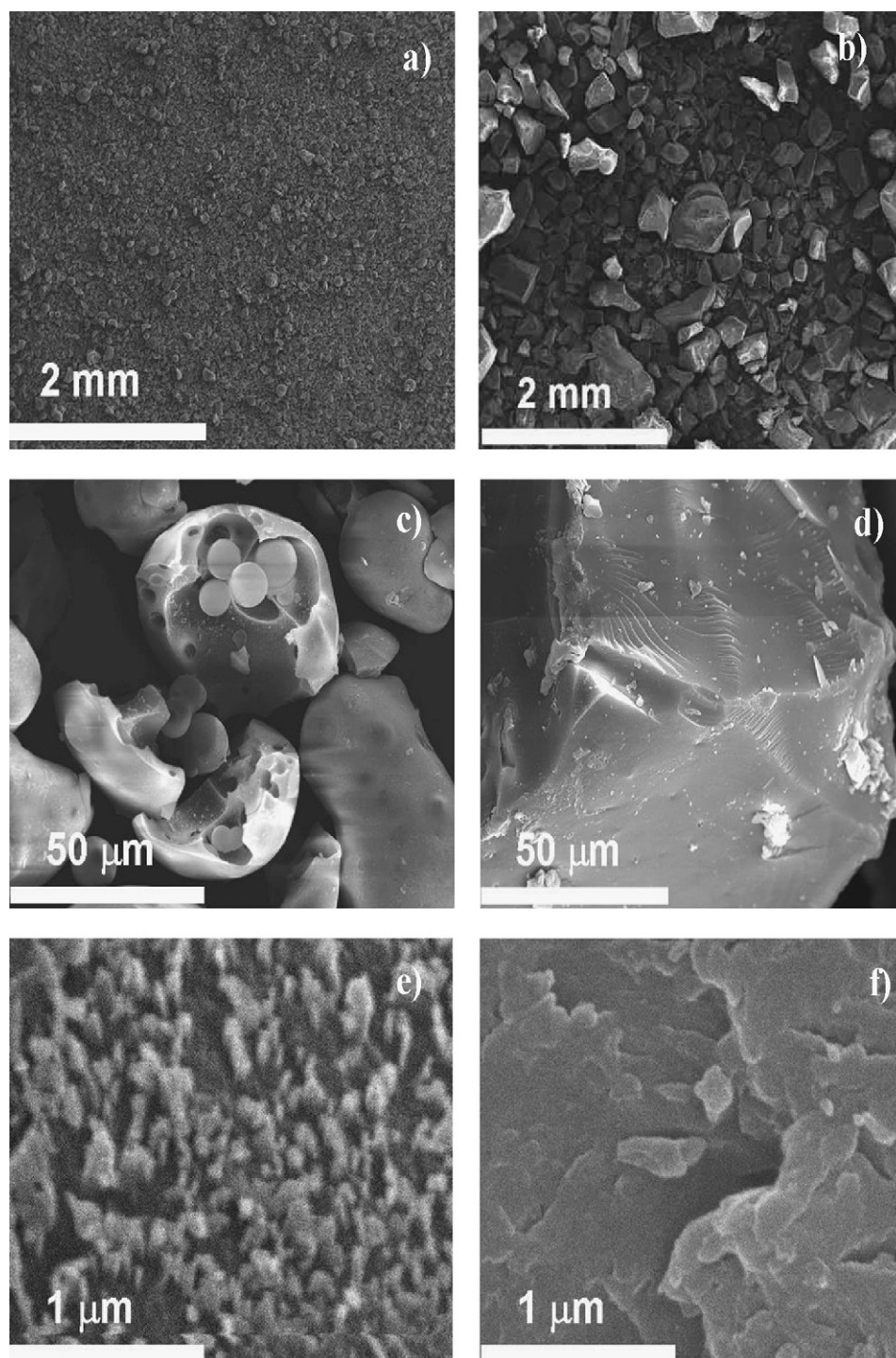


Fig. 2. SEM images of KL (a, c and e) and KL<sub>d</sub> (b, d and f) at different magnifications.

Table 2  
Carbon yield on daf basis, and proximate and ultimate analyses of the ACs prepared from KL and KL<sub>d</sub>

T (°C)	Yield <sup>a</sup>	Proximate analysis (wt.%, dry basis)			Ultimate analysis (wt.%, daf)				
		Volatile matter	Fixed carbon	Ash	C	H	N	S	O
<b>KL</b>									
400	87.6	35.08	64.14	0.78	65.3	1.2	0.0	1.0	32.5
500	85.0	31.23	67.11	1.66	70.2	1.1	0.0	1.1	27.6
600	65.7	30.99	58.15	3.00	72.7	0.5	0.0	1.2	25.6
<b>KL<sub>d</sub></b>									
400	80.9	35.90	64.06	0.04	61.4	1.2	0.0	1.0	36.4
500	73.3	34.52	65.42	0.06	62.7	1.1	0.0	0.7	35.5
600	61.3	32.42	67.48	0.10	63.5	0.8	0.0	0.6	35.1

<sup>a</sup> Dry ash-free basis.

phenol to aliphatic hydroxyl ratio, and a decrease of the total hydroxyl content of the lignin.

Fig. 2 shows SEM images of KL and KL<sub>d</sub> at different magnifications. Differences in particle shapes and sizes may be observed. KL particles are smaller, and have a rounded (even spherical) shape with widely open volumes inside. Such a morphology is probably a result of the concentration process of lignin from black liquors, which is done by evaporation; due to their surface tension, the particles take a spherical – thermodynamically more stable – form. After acid washing, the KL<sub>d</sub> particles are much bigger and sharp, and look broken. A more detailed observation reveals that the surface of the KL particles is rough, whereas that of the KL<sub>d</sub> is nearly smooth. Such a different morphology between KL and KL<sub>d</sub> is probably due to the method used for lignin separation (evaporation or sedimentation–filtration) although changes in the polymer structure due to the demineralisation process cannot be excluded.

### 3.2. Characterisation of the produced activated carbons

#### 3.2.1. Carbon yield and elemental composition

Table 2 shows the carbon yield (daf basis) and the proximate and ultimate analyses of the prepared activated carbons. Yields in carbon are always higher from KL than from KL<sub>d</sub>, ranging from 65.7 to 87.6% and from 61.3 to 80.9%, respectively. Additionally, their dependence on temperature is not the same. Increasing the temperature from 400 to 500 °C makes the carbon yield decrease by 2.6 and 7.6% for KL and KL<sub>d</sub>, respectively. On the contrary, within the range 500–600 °C, the carbon yield decreases much more for KL (19.3%) than for KL<sub>d</sub> (12.0%).

PA promotes dehydration, producing an important reordering of the structure [29], decreasing the amount of volatile compounds emitted during decomposition and hence increasing the carbon yield. Our previous works [30,31] also showed that, during thermal decomposition, the PA-impregnated lignin follows a reaction path which is different from that observed with pure lignin, and that the carbon yield is higher. PA promotes bond cleavage in the biopolymers and dehydration at low temperatures [32] followed by extensive cross-linking that binds volatile matter into the carbon product, and thus increases the carbon yield. Consequently, activated carbons may be prepared with good yields and high surface areas using chemical activation

with PA. Since demineralisation decreases the hydroxyl content of lignin, the reaction of PA with lignin – and so the subsequent cross-linking – are clearly lowered. Therefore, the aromaticity of the activated carbons and the carbon yield also decrease.

Fig. 3 shows the Van Krevelen diagram, plotting H/C versus O/C ratios, for activated carbons derived from KL and KL<sub>d</sub> within the temperature range of this study. The ACs become increasingly more aromatic when the temperature increases, but such a variation depends on the precursor. At constant pyrolysis temperature, ACs derived from KL have lower H/C and O/C ratios than those prepared from KL<sub>d</sub>, suggesting a higher aromatic nature that increases with temperature. The Van Krevelen diagram confirms the lower aromaticity of the ACs prepared from KL<sub>d</sub>. Furthermore, it is not excluded that the acid pretreatment could form new polymeric structures that would be thermally less resistant, resulting in a decrease of the carbon yield.

#### 3.2.2. Surface area and porosity

Table 3 shows the BET surface area and the porosity of carbons produced from KL and KL<sub>d</sub> at 400, 500 and 600 °C. The maximum surface area determined in this work, 1189 m<sup>2</sup>/g, corresponds to the carbon prepared from KL at 600 °C. All the surface areas determined by the BET method are higher than 800 m<sup>2</sup>/g, but the observed temperature dependences are very different for carbons prepared from KL and KL<sub>d</sub>. The surface areas increase with carbonisation temperature for KL-based carbons while the opposite is observed for those prepared from

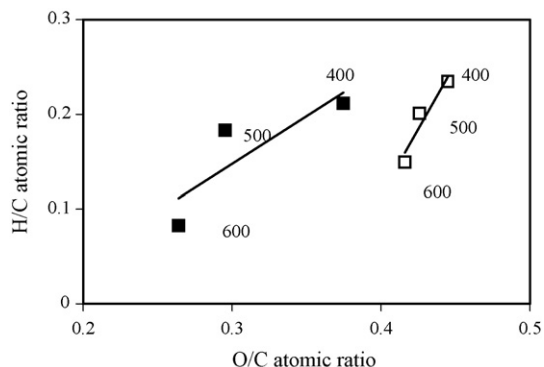


Fig. 3. Van Krevelen diagram for ACs prepared from KL (full symbols) and KL<sub>d</sub> (open symbols) at 400, 500 and 600 °C.

Table 3

Textural parameters of activated carbons prepared from KL and KL<sub>d</sub>, deduced from N<sub>2</sub> adsorption at 77 K

T (°C)	A <sub>BET</sub> (m <sup>2</sup> /g)	V <sub>0.99</sub> (cm <sup>3</sup> /g)	DR equation			α <sub>s</sub> method	
			V <sub>DR</sub> (cm <sup>3</sup> /g)	E <sub>0</sub> (kJ/mol)	L <sub>0</sub> (nm)	V <sub>micro</sub> (cm <sup>3</sup> /g)	V <sub>ultra</sub> (cm <sup>3</sup> /g)
KL as carbon precursor							
400	815	0.40	0.38	22.2	1.0	0.34	0.18
500	1004	0.49	0.45	19.7	1.3	0.43	0.13
600	1189	0.59	0.51	18.9	1.5	0.49	0.11
KL <sub>d</sub> as carbon precursor							
400	1008	0.47	0.45	19.1	1.4	0.45	0.12
500	960	0.46	0.40	17.9	1.7	0.38	0.05
600	890	0.44	0.37	17.6	1.7	0.35	0.04

KL<sub>d</sub>. The same trends are observed for the variation of V<sub>DR</sub> and V<sub>micro</sub>. However, the volume of pores narrower than 0.7 nm determined by the α<sub>s</sub> method, V<sub>ultra</sub>, decreases with increasing temperature for all the carbons prepared. V<sub>ultra</sub> is always the highest for carbons prepared from KL, and its decrease (from 0.18 to 0.11 cm<sup>3</sup>/g) is less than that observed for carbons prepared from KL<sub>d</sub> (from 0.12 to 0.04 cm<sup>3</sup>/g) when the temperature increases from 400 to 600 °C. Finally, the average micropore width derived from the DR method, L<sub>0</sub>, increases with the temperature, whatever the material, although higher values were found with KL<sub>d</sub>.

The results of the present study show that, on average, the adsorbents made from KL have better characteristics (higher areas and pore volumes) than those derived from KL<sub>d</sub>. Such differences between KL and KL<sub>d</sub> may be explained by the ability of PA to react with lignin. KL can react more extensively with PA due to its higher phenolic content. Moreover, the deashed lignin is less reactive (much more compact, as revealed by SEM, and with much less hydroxyl groups with which PA can react, as revealed by IR spectra), due to an acid-induced cross-linking of the macromolecules. PA can penetrate easily the texture of KL, producing an increasingly high number of small micropores when the temperature increases. Additionally, phosphate and polyphosphate bridges connect cross-linked biopolymer fragments, avoiding pore collapse. On the contrary, PA hardly penetrates KL<sub>d</sub>, and cannot prevent pore collapse; hence, the activation mainly occurs at the surface of the grains, producing wider pores (higher L<sub>0</sub> and lower E<sub>0</sub> than for KL). Finally, a catalytic effect of cations improving the activation at constant temperature is also possible.

### 3.2.3. Surface chemistry of the activated carbons

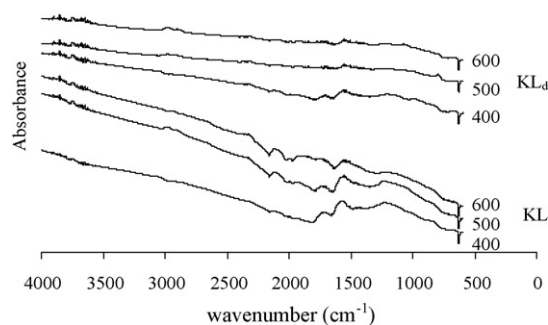
Fig. 4 shows the FT-IR spectra of the ACs derived from KL and KL<sub>d</sub>. The band around 1700 cm<sup>-1</sup> is usually caused by the stretching vibration of C=O in ketones, aldehydes, lactones, and carboxyl groups, and the band around 1600 cm<sup>-1</sup> is ascribed to aromatic ring stretching vibrations. The intensities of these two bands clearly show that the aromaticity and the carbonyl groups content are much higher in ACs derived from KL than in those prepared from KL<sub>d</sub>. The band around 1230 cm<sup>-1</sup> is usually attributed to C–O bonds; however, in carbons activated by H<sub>3</sub>PO<sub>4</sub>, the bands at 1300–900 cm<sup>-1</sup> could also be caused by phosphorus-containing groups [33].

Spectra of ACs prepared from KL<sub>d</sub> are much smoother than those of ACs prepared from KL, evidencing a lower amount of functional groups. It may also be observed that, for both types of carbons, increasing the temperature reduces the intensity of all the bands. In a recent study [18], it has been demonstrated that the acidic groups at the surface of carbons prepared from Kraft lignin can be temperature-sensitive or not, depending on their chemical composition. The temperature-sensitive functions mainly consist of carbonyl-containing groups of various acidic strengths, while the temperature-insensitive groups mainly comprise phosphorus. Thus, the functional groups of the ACs prepared from KL<sub>d</sub> would be essentially temperature-sensitive, whereas those prepared from KL would include temperature-sensitive and temperature-insensitive (i.e., containing phosphorus) groups, due to the more extensive reaction of PA with KL. These findings are in good agreement with the results on MB adsorption, given below.

### 3.2.4. MB adsorption

Fig. 5 shows the dependence of the MB adsorption capacity of the ACs on the concentration of acidic surface functions, expressed in meq H<sup>+</sup>/m<sup>2</sup>. The MB adsorption capacity decreases as the surface acidity increases, for both kinds of carbons prepared from KL and KL<sub>d</sub>. Thus, increasing the number of acidic groups or decreasing the surface area lowers the adsorption of MB.

Concerning the effect of acidic groups, it is known that when a porous carbon comes into contact with a MB solution, water first adsorbs on the hydrophilic polar oxygen groups, including those located at the micropore entrance [34,35]. Water molecules indeed can form H-bonding with surface oxygen groups [36,37],

Fig. 4. FT-IR spectra of ACs prepared from KL and KL<sub>d</sub> at 400, 500 and 600 °C.

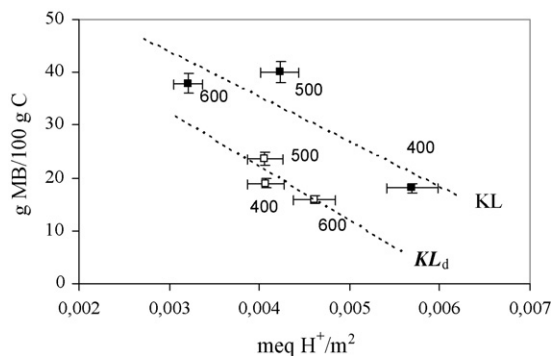


Fig. 5. Methylene blue (MB) adsorption capacity vs. concentration of acidic surface functions (meq H<sup>+</sup>/m<sup>2</sup>) of the ACs prepared from KL (full symbols) and KL<sub>d</sub> (open symbols) at 400, 500 and 600 °C.

and are more strongly adsorbed than MB on such sites [38], especially at neutral pH and extremely low concentration of MB [39]. The adsorbed water molecules further associate with each other to form clusters [37–40] which are remarkably stabilised in micropores [41], causing the partial blockage of their entrance, reducing the accessible surface area [38,42], and finally hindering or even preventing MB adsorption area [35,43]. Another explanation of the low MB adsorption capacity of ACs containing a higher number of acidic surface groups is based on electron density considerations. The electronegativity of the oxygen atoms induces the polarisation of the carbon surface and the subsequent depletion of the electron density inside the aromatic rings, which leads to a decrease in the strength of the interactions between the aromatic rings of the organic molecule and the carbon basal planes. An overall effect is a decrease in the average energy of adsorption for MB molecules and thus, the decrease in the corresponding adsorbed amount [44,45].

Increasing the preparation temperature of the ACs leads to materials having less oxygen-containing groups. The opportunity of forming water clusters is thus lowered, giving a higher accessibility of the pores to MB molecules, and improving the interaction potential between MB molecules and the carbon surface. Consequently, the adsorption of water on the surface of samples prepared at higher temperature is lower, while that of MB molecules is improved. However, in Section 3.2.2, the temperature was shown to produce opposite effects on the change of pore texture, depending on how the activated carbons were prepared (see again Table 3). The surface area of carbons prepared from KL<sub>d</sub> was indeed seen to decrease with the temperature, while that of materials made from KL was seen to increase. As a consequence, MB adsorption increases with the activation temperature for carbons prepared from KL, whereas the opposite trend is observed, in average, for those prepared from KL<sub>d</sub> (see Fig. 5).

Moreover, carbons from KL present higher MB adsorption capacities than those from KL<sub>d</sub>, even when having similar surface areas. Fig. 5 shows that straight and almost parallel lines may be fitted to the data of MB adsorption capacities of both kinds of ACs. Such a behaviour could be ascribed to the different nature of the acidic surface groups (carbons from KL presenting more phosphoric acidic groups), but also to the higher aromaticity

of the ACs from KL promoting dispersive interactions between aromatic rings of MB molecules and basal (also aromatic) planes of carbon. However, as showed by Karaca et al. [46], the effect of the ash content may play an even more important role on MB adsorption. These authors showed that carbonate and silicate minerals, together with the presence of organic sulphur inside the carbon matrix, have a positive effect on methylene blue adsorption. Improvement of MB adsorption due to the sulphur present in chars derived from the carbonisation of tires has also been observed by Helleur et al. [47]. Table 2 indeed confirms that ACs prepared from KL, presenting the highest MB adsorption capacity, are also those containing the highest level of sulphur (up to two times the S content of ACs derived from KL<sub>d</sub>, when prepared at 600 °C).

#### 4. Conclusions

The objective of this work was to study the effect of the ash content of softwood Kraft lignin on the properties of the activated carbons produced by activation with H<sub>3</sub>PO<sub>4</sub> (PA). SEM observations and IR studies suggest that the demineralisation process produces lignin polymerisation and reduces its ability to react with PA.

The results have shown that carbon yield, surface area, porosity and surface chemistry are affected by the removal of the mineral matter. The activated carbons prepared by activation of KL and KL<sub>d</sub> are essentially microporous with surface areas higher than 800 m<sup>2</sup>/g, the highest one being close to 1200 m<sup>2</sup>/g and corresponding to the AC prepared from KL at 600 °C. The carbon yield and the aromaticity are the highest for activated carbons derived from the raw Kraft lignin (KL). The surface area increases with temperature for ACs prepared from KL, but the opposite trend is observed for those prepared from KL<sub>d</sub>. The number of functional groups decreases when temperature increases, and is the highest for the ACs prepared from KL, probably because they contain more phosphorus-based groups, which have been recently described as temperature-insensitive. MB adsorption is higher for ACs prepared from KL, mainly because of their higher ash and sulphur contents.

In other words, it may be concluded that the very different characteristics of the KL- or KL<sub>d</sub>-based ACs may clearly be attributed to the demineralisation process itself. However, a favourable catalytic effect of the ashes on the activation process could not be discarded.

The main conclusion of this work is then the following: since better active carbons are produced from raw lignin, the demineralisation – if required – should be carried out on the products and not on the precursors.

#### Acknowledgements

This research was partly made possible by financial support from MCYT (project PPQ2002-04201-CO02), DURSI (2001SGR00323) and the European Commission through the ALFA program (project LIGNOCARB-ALFA II 0412 FA FI). V. Fierro acknowledges the financial support of her ‘Ramón y Cajal’ research contract (2002–2005) by the MCYT and the Uni-

versitat Rovira i Virgili (URV). V. Torné-Fernández thanks the URV for her PhD grant.

## References

- [1] J. Rodríguez-Mirasol, T. Cordero, J.J. Rodríguez, Preparation and characterization of activated carbons from eucalyptus kraft lignin, *Carbon* 31 (1993) 87–95.
- [2] E. González-Serrano, T. Cordero, J. Rodríguez-Mirasol, J.J. Rodríguez, Development of porosity upon chemical activation of kraft lignin with  $ZnCl_2$ , *Ind. Eng. Chem. Res.* 36 (1997) 4832–4838.
- [3] J. Hayashi, A. Kazehaya, K. Muroyama, A.P. Watkinson, Preparation of activated carbon from lignin by chemical activation, *Carbon* 38 (2000) 1873–1878.
- [4] V. Fierro, V. Torné-Fernández, A. Celzard, Kraft lignin as a precursor for microporous activated carbons prepared by impregnation with *ortho*-phosphoric acid: synthesis and textural characterisation, *Micropor. Mesopor. Mater.* 92 (2006) 243–250.
- [5] M.V. Rivera-Utrilla, López-Ramón, F. Carrasco-Marín, F.J. Maldonado-Hódar, C. Moreno-Castilla, Demineralization of a bituminous coal by froth flotation before obtaining activated carbons, *Carbon* 34 (1996) 917–921.
- [6] C. Bansal, J.B. Donnet, H.F. Stoeckli, *Active Carbon*, Marcel Dekker, New York, 1988.
- [7] F. Kapteijn, H. Porre, J.A. Moulijn,  $CO_2$  gasification of activated carbon catalyzed by earth alkaline elements, *AIChE J.* (1986) 691–695.
- [8] D. Fengel, G. Wegener, *Wood: Chemistry Ultrastructure, Reactions*, Walter de Gruyter, New York, 1984, pp. 132–181.
- [9] J.G. Spreigh, *Chemistry and Technology of Coal*, Marcel Dekker, New York, 1994.
- [10] D.W. Van Krevelen, *Coal*, Elsevier, Amsterdam, 1993.
- [11] M. Kleen, G. Gellerstedt, Influence of inorganic species on the formation of polysaccharide and lignin degradation products in the analytical pyrolysis of pulps, *J. Anal. Appl. Pyrol.* 35 (1995) 15–41.
- [12] E. Jakab, O. Faix, F. Till, Thermal decomposition of milled wood lignins studied by thermogravimetry/mass spectrometry, *J. Anal. Appl. Pyrol.* 40 (1997) 171–186.
- [13] J.C. Rio, A. Gutierrez, J. Romero, M.J. Martinez, T. Martinez, Identification of residual lignin markers in eucalypt kraft pulps by Py–GC/MS, *J. Anal. Appl. Pyrol.* 58–59 (2001) 425–439.
- [14] R.K. Sharma, J.B. Wooten, V.L. Baliga, X. Lin, W.G. Chan, M.R. Hajaligol, Characterization of chars from pyrolysis of lignin, *Fuel* 83 (2004) 1469–1482.
- [15] W.F. DeGroot, F.J. Shafizadeh, The influence of exchangeable cations on the carbonization of biomass, *J. Anal. Appl. Pyrol.* 6 (1984) 217–232.
- [16] L. Khezami, A. Chetouani, B. Taouk, R. Capart, Production and characterisation of activated carbon from wood components in powder: cellulose, lignin, xylan, *Powder Technol.* 157 (2005) 48–56.
- [17] E. González-Serrano, T. Cordero, J. Rodríguez-Mirasol, L. Cotoruelo, J.J. Rodríguez, Removal of water pollutants with activated carbons prepared from  $H_3PO_4$  activation of lignin from kraft black liquors, *Water Res.* 38 (2004) 3043–3050.
- [18] Y. Guo, D.A. Rockstraw, Physical and chemical properties of carbons synthesized from xylan, cellulose, and Kraft lignin by  $H_3PO_4$  activation, *Carbon* 44 (2006) 1464–1475.
- [19] J. Rodríguez-Mirasol, J. Bedia, T. Cordero, J.J. Rodríguez, Influence of water vapor on the adsorption of VOCs on lignin-based activated carbons, *Sep. Sci. Technol.* 40 (2005) 3113–3135.
- [20] F. Rouquerol, J. Rouquerol, K.S.W. Sing, *Adsorption by Powders and Porous Solids. Principles, Methods and Applications*, Academic Press, San Diego, CA, 1999.
- [21] N. Setoyama, T. Suzuki, K. Kaneko, Simulation study on the relationship between a high resolution  $\alpha_s$ -plot and the pore size distribution for activated carbon, *Carbon* 36 (1998) 1459–1467.
- [22] C.H. Hoyt, D.W. Goheen, in: K.V. Sarkanen, C.H. Ludwig (Eds.), *Lignins*, Wiley-Interscience, New York, 1971, p. 833.
- [23] E. Papirer, E. Guyon, N. Perol, Contribution to the study of the surface groups on carbons. II. Spectroscopic methods, *Carbon* 16 (1978) 133–140.
- [24] D. Fengel, G. Wegener, *Wood. Chemistry Ultrastructure Reactions*, De Gruyter, 1989, pp. 143–164.
- [25] G. Socrates, *Infrared Characteristic Group Frequencies*, John Wiley & Sons, 1980.
- [26] C.G. Boeriu, D. Bravo, R.J.A. Gosselink, J.E.G. van Dam, *Ind. Crops Prod.* 20 (2004) 205–218.
- [27] S. Yasuda, N. Terashima, T. Ito, Chemical structure of sulfuric acid lignin I. Chemical structures of condensation products from monolignols, *Mokuzai Gakkaishi* 26 (1980) 552–557.
- [28] S. Yasuda, K. Hayashi, T. Ito, N. Terashima, Chemical structures of hydrochloric acid lignin I. Chemical structures of condensation products from monolignols, *Mokuzai Gakkaishi* 27 (1981) 478–483.
- [29] Y.Z. Lai, in: D.N.S. Hon, N. Shirashi (Eds.), *Wood and Cellulosic Chemistry*, vol. 10, Marcel Dekker, New York, 1991, p. 455.
- [30] D. Montané, V. Torné-Fernández, V. Fierro, Activated carbons from lignin: kinetic modeling of the pyrolysis of Kraft lignin activated with phosphoric acid, *Chem. Eng. J.* 106 (2005) 1–12.
- [31] V. Fierro, V. Torné-Fernández, D. Montané, A. Celzard, Study of the decomposition of kraft lignin impregnated with orthophosphoric acid, *Therm. Acta* 433 (2005) 142–148.
- [32] M. Jagtoyen, F. Derbyshire, Some considerations of the origins of porosity in carbons from chemically activated wood, *Carbon* 31 (1993) 1185–1192.
- [33] M. Puziy, O.I. Poddubnaya, A. Martínez-Alonso, F. Suárez-García, J.M.D. Tascón, Synthetic carbons activated with phosphoric acid. I. Surface chemistry and ion binding properties, *Carbon* 40 (2002) 1493–1505.
- [34] S.K. Verma, P.L. Walker, Alteration of molecular sieving properties of microporous carbons by heat treatment and carbon gasification, *Carbon* 28 (1990) 175–184.
- [35] P. Pendleton, S.H. Wu, A. Badalyan, Activated carbon oxygen content influence on water and surfactant adsorption, *J. Colloid Interf. Sci.* 246 (2002) 235–240.
- [36] R. Coughlin, F.S. Ezra, Role of surface acidity in the adsorption of organic pollutants on the surface of carbon, *Environ. Sci. Technol.* 2 (1968) 291–297.
- [37] T. Iiyama, M. Ruike, K. Kaneko, Structural mechanism of water adsorption in hydrophobic micropores from in situ small angle X-ray scattering, *Chem. Phys. Lett.* 331 (2000) 359–364.
- [38] M. Franz, H.A. Arafat, N.G. Pinto, Effect of chemical surface heterogeneity on the adsorption mechanism of dissolved aromatics on activated carbon, *Carbon* 38 (2000) 1807–1819.
- [39] A.P. Terzyk, Molecular properties and intermolecular forces—factors balancing the effect of carbon surface chemistry in adsorption of organics from dilute aqueous solutions, *J. Colloid Interf. Sci.* 275 (2004) 9–29.
- [40] D. Mowla, D.D. Do, K. Kaneko, Adsorption of water vapor on activated carbon: a brief overview, in: L.R. Radovic (Ed.), *Chemistry and Physics of Carbon*, vol. 28, Marcel Dekker, New York, 2003, pp. 229–262.
- [41] T. Ohba, H. Kanoh, K. Kaneko, Affinity transformation from hydrophilicity to hydrophobicity of water molecules on the basis of adsorption of water in graphitic nanopores, *J. Am. Chem. Soc.* 126 (2004) 1560–1562.
- [42] C. Moreno-Castilla, Adsorption of organic molecules from aqueous solutions on carbon materials, *Carbon* 42 (2004) 83–94.
- [43] I.I. Salame, T.J. Bandoz, Study of water adsorption on activated carbons with different degrees of surface oxidation, *J. Colloid Interf. Sci.* 210 (1999) 367–374.
- [44] L.R. Radovic, I.F. Silva, J.I. Ume, J.A. Menendez, C.A. Leon y Leon, W.A. Scaroni, An experimental and theoretical study of the adsorption of aromatics possessing electron-withdrawing and electron-donating functional groups by chemically modified activated carbons, *Carbon* 35 (1997) 1339–1348.
- [45] I.I. Salame, T.J. Bandoz, Role of surface chemistry in adsorption of phenol on activated carbons, *J. Colloid Interf. Sci.* 264 (2003) 307–312.
- [46] S. Karaca, A. Gürses, R. Bayrak, Effect of some pre-treatments on the adsorption of methylene blue by Balkaya lignite, *Energy Conv. Manag.* 45 (2004) 1693–1704.
- [47] R. Helleur, N. Popovic, M. Ikura, M. Stanculescu, D. Liu, Characterization potential applications of pyrolytic char from ablative pyrolysis of used tires, *J. Anal. Appl. Pyrol.* 58–59 (2001) 813–824.